Korean J. Chem. Eng., 36(11), 1890-1899 (2019)
DOI: 10.1007/s11814-019-0379-7

pISSN: 0256-1115
eISSN: 1975-7220

Influence of the parameters of chitin deacetylation process on the chitosan obtained from crab shell waste

Carla-Cezarina Pădureţu*, Raluca Isopescu, Ileana Rău*,†, Manuela Rossemary Apetroaei***, and Verginica Schröder****

*University POLITEHNICA of Bucharest, Faculty of Applied Chemistry and Materials Science, Department of General Chemistry, 1-7 Polizu Str., 011061, Bucharest, Romania
**University POLITEHNICA of Bucharest, Faculty of Applied Chemistry and Materials Science, Department of Chemical and Biochemical Engineering, 1-7 Polizu Str., 011061, Bucharest, Romania
***"MIRCEA CEL BATRAN" Naval Academy, Department of Naval and Port Engineering and Management, Faculty of Navigation and Naval Management, 1 Fulgerului Str., 900218, Constanta, Romania
****University OVIDIUS of Constanta, Faculty of Pharmacy, 1 University Str., C Building Campus, 900470, Constanta, Romania
(*Received 11 July 2019 • accepted 28 August 2019*)

Abstract−Chitosan, one of the most interesting and intriguing biopolymer, can be extracted from different marine waste. The present paper focuses on the chitosan extraction procedure from *Macropipus holsatus* crab waste. Because the deacetylation degree is the most important characteristic of chitosan, the influence of specific operating parameters during deacetylation treatment was analyzed by statistical analysis and mathematical modelling using artificial neural networks (ANN). The ANN simulation put into evidence the manner that the deacetylation degree is influenced by the considered operating conditions and enabled the identification of optimal operating conditions in order to obtain a chitosan with a relatively high deacetylation degree. The obtained chitosan was characterized by various methods, including physical-chemical analysis, structure identification and crystallinity index. The main effects as well as the interaction effects for some physical-chemical properties were studied to establish if and how the chitosan properties are affected by the extraction procedure.

Keywords: Crabs, Chitin, Chitosan, Deacetylation Degree, *Macropipus holsatus*

INTRODUCTION

Chitosan, which is a natural polysacharide very widespread in nature [1], represents the *N*-deacetylated derivative of chitin [2]. Chitosan is a copolymer composed of randomly distributed units of 2-amino-2-deoxy-D-glucopyranose and 2-acetamide-2-deoxy-D-glucopyranose linked by (1,4)-β-glycosidic bonds [3-5]. It is commonly found in marine invertebrates such as crustacean exoskeletons and molluscs. At the same time, cuticles of insects, certain fungi and algae could contain chitin [3,6]. The chemical structures of chitin and chitosan are presented in Fig. 1.

α-Chitin is the most abundant crystalline form occurring in nature and it is often found in the shell of crustaceans and fungi cell walls [8]. Generally, chitin is a rigid material with highly ordered hydrogen bonds between chains. This structure determines the specific properties like high crystallinity, poor solubility, swelling behavior and low reactivity [9]. On the other hand, chitosan readily dissolves in aqueous solution of some organic acids such as acetic, lactic or citric at pH values less than 6.3 [6], when the free amino groups are protonated having as consequence a higher solubility [10]. It was proved that chitosan and also chitosan composites are efficient materials that could be used in different environmental activities due to the heavy metal removal capacity [11-13] and sorption capacity [14]. Chitosan's properties could be succesfully en-

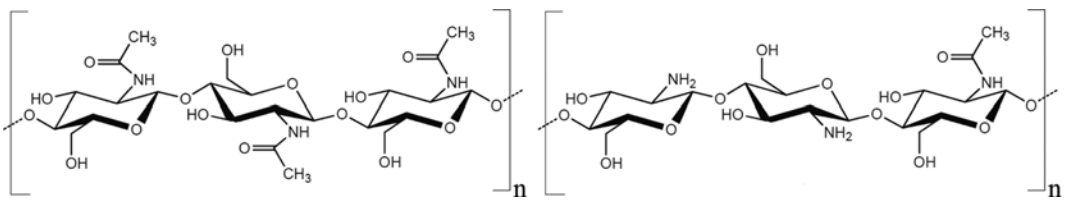

Fig. 1. Chemical structure of chitin (left) and chitosan (right) (adapted from [7]).

†To whom correspondence should be addressed.
E-mail: ileana_brandusa@yahoo.com

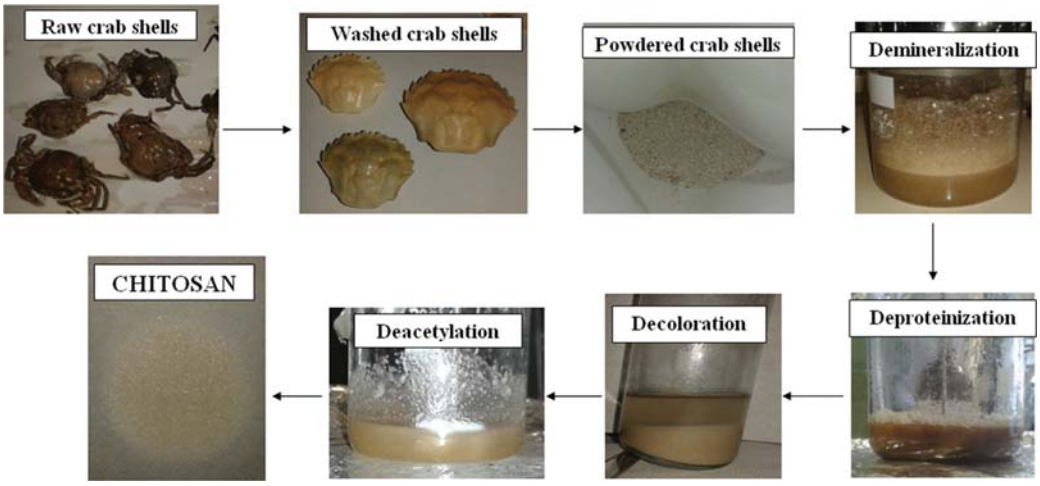

Fig. 2. General scheme of chitin extraction and chitosan production.

hanced by blending it with different other materials [15-17] that could also be converted into membranes depending on the applications field [2,18].

Chitosan optimization studies were previously conducted for the processes using shrimp waste [19-23] and fish scales [24], but optimization of chitosan production from crabs was less studied [25]. Crabs have a higher mineral content compared to shrimps or lobster [26], which may influence the chitin deacetylation process.

The solubility is closely associated with the deacetylation degree and the molar mass [27], mostly because chitosan is in fact a mixture of two polymers (chitin and chitosan) with different solubility behavior [28]. Increasing the deacetylation degree leads to a high content of chitosan having as result more amino groups and therefore an increasing solubility in acetic acid solutions is expected. At the same time, chitosan solubility behavior is influenced by the molar mass of chitosan through the intrinsic viscosity of chitosan solutions [29].

The aim of the present paper was to study the variability of the extraction process for chitin deacetylation and characterization of the chitosan obtained from *Macropipus holsatus* crab species. An artificial neural network modeling technique was used to estimate the optimum conditions that could lead to a high deacetylation degree chitosan product, and the optimization was carried out using genetic algorithms implemented in MATLAB©.

EXPERIMENTAL PART

1. Material Characterization

The crab species chosen for the present study is *Macropipus holsatus* (Fabricius, 1798), also known as *Liocarcinus holsatus* (Fabricius, 1798) or the flying swimming crab [30,31]. It is one of the most widely distributed species on the Black Sea sand beaches, having a specific color, sandy or grayish-green, depending on the living area [32]. The carapace of *Liocarcinus holsatus* is recognized by its smoothness, without crenulated ridges and presents three frontal strong teeth and four distinctive teeth on the anterolateral margin. Last pair of legs is paddle-shaped, adapted for swimming purposes, being wider and more flattened than the segments of previous legs. The species has strong but short basal article of antennae [32,33]. Crabs of *Macropipus holsatus* (Fabricius, 1798) species were collected as waste from the Romanian Black Sea Coast, in Mamaia area (44°18′N/028°63′E) in July 2017.

Chitin and chitosan from ChromaDex (LGC Standards, Wesel, Germany), as well as chitosan purchased from Sigma-Aldrich (DD= 75-85%, M_w=50-190 kDa in 1% acetic acid solution), were used for comparison. Hydroxide solutions were prepared using NaOH pellets with purity higher than 99.3% purchased from ChimReactiv S.R.L.

2. Extraction Method

The chitin extraction procedure and chitosan production steps are presented in Fig. 2.

Demineralization was carried out in HCl 4%, at a solvent-to-solid ratio of 15 : 1 (v : w) for 1 hour at room temperature, under continuous stirring, where 81.34% of the mineral salts was considered as loss material. The next step, deproteinization, consisted in using NaOH 3%, at a solvent-to-solid ratio of 20 : 1 (v : w) for 2 hours at 65 °C, under continuous stirring, where 6.43% of the proteins was considered as loss material. Because the exoskeleton of crustacea naturally contains colorants such as astaxanthin and β-carotene [6], a depigmentation treatment was required. The decoloration procedure was conducted at room temperature using acetone in a 1 : 1 (v : w) solvent-to-solid ratio, and the obtained material was rinsed with bidistilled water for three times; the chitin yield was 12.23% of the initial mass considered for the experiments. Further, chitin deacetylation process was performed at 95-100 °C with parameters varying according to Table 1. After each of the treatments presented above, the obtained material was rinsed with bidistilled water until neutral pH was reached and dried until constant mass. Overall, a chitosan yield of 9.52% (related to the raw material used) was obtained.

The experiment type was unreplicated factorial, according to Montgomery [34]. Table 1 presents the experimental deacetylation parameters for chitosan preparation from *Macropipus holsatus* crab. The values corresponding for the maximum (+1) and minimum (−1) factors were chosen based on the literature data [6,19,22,29]. Therefore, for deacetylation time the maximum was selected 100

Table 1. Experimental deacetylation parameters for chitosan preparation from *Macropipus holsatus* crab

Experiment/ Sample no.	Factor A		Factor B		Factor C	
	x_1	Contact time at 100 °C, min	x_2	NaOH solvent-to-solid ratio, v : w	x_3	NaOH concentration, %
1.	−1	60	−1	10 : 1	−1	40
2.	+1	100	−1	10 : 1	−1	40
3.	−1	60	+1	20 : 1	−1	40
4.	+1	100	+1	20 : 1	−1	40
5.	−1	60	−1	10 : 1	+1	50
6.	+1	100	−1	10 : 1	+1	50
7.	−1	60	+1	20 : 1	+1	50
8.	+1	100	+1	20 : 1	+1	50
9.	0	80	0	15 : 1	0	45
10.	0	80	0	15 : 1	0	45

and the minimum 60 min, for NaOH solvent-to-solid ratio 20 : 1 v : wt, respectively 10 : 1 v : wt and for NaOH concentration 50%, respectively, 40%. In these conditions the central point (0) was considered deacetylation time 80 min, NaOH solvent-to-solid ratio 15 : 1 v : wt and NaOH concentration 45%. Two replicates were performed in the center of the program to evaluate the experimental error during the deacetylation process of chitin. To study the variability of the process, the main effects as well as the interaction effects were determined.

3. Physical-chemical Characterization of Chitosan

The deacetylation degree (DD) of chitosan samples was determined by potentiometric pH-measurements and the end of titration was indicated by the presence of two inflection points. The first inflection point corresponds to the neutralization of the excess protons from hydrochloric acid, while the difference between the second one and the first one corresponds to the amount of NaOH needed for reaction with H^+ of amine groups [35]. The value of DD (%) was calculated according to equation [36]:

$$DD(\%) = \frac{(203 \times Q)}{(1 + 42 \times Q)} \quad (1)$$

$$\text{where: } Q = \frac{c_M \times \Delta V}{m} \quad (2)$$

c_M represents the molar concentration of NaOH solution used for titration (mol/L); ΔV is the volume difference between the two inflection points (L); m is the mass of the analyzed chitosan (g); 203 represents the molar mass of chitin (g/mol) and 42 is the molar mass of acetyl group (g/mol).

The average molar mass determination was performed for chitosan solutions prepared in 2% acetic acid and 0.1 M KCl [37] using a micro-Ostwald viscometer purchased from SI Analytics GmbH™, Type No. 285404409, 518 10 model, with capillary tube inner diameter of $Ø_i$=0.43 mm. The measurements were performed at 25± 1 °C. The average molar mass was determined using the Mark-Houwink equation:

$$[\eta] = K \times \overline{M}^{\alpha} \quad (3)$$

where: $[\eta]$ represents intrinsic viscosity (mL/g); $\overline{M}$ is the average molar mass (Da) while K and α are constants depending on the polymer and the solvent used for determination analysis (K= 0.0138 mL/g, α=0.85 [38]).

Solubility was determined using a modified method of Fernandez-Kim [39]. Chitosan samples were dissolved in acetic acid 1% in a ratio of acetic acid-to-solid of 100 : 1 (v : w), shaken in a vortex mixer for 15 min and then immersed in a hot water bath at 60 °C for 10 min. The samples were cooled to room temperature (25 °C) and centrifuged at 10 000 rpm for 10 min. The supernatant was discarded and the solution was washed with bidistilled water and centrifuged at 10 000 rpm. The samples were dried at 60 °C for 24 h and the solubility percentage was determined using the following equation:

$$S(\%) = \frac{m_i - m_f}{m_i} \times 100 \quad (4)$$

where: m_i is the initial mass of chitosan and m_f represents the final mass of chitosan.

Moisture content (M) of the samples kept in atmospheric conditions was determined according to AOAC 2000 standard [40] at 105±1 °C using the following Eq. (5):

$$\text{Moisture}(\%) = \frac{w_i - w_f}{w_i} \times 100 \quad (5)$$

where: w_i represents the mass of the sample before drying (g) while w_f represents the mass of the sample after drying (g).

The chemical analyses for DD, average molar mass, solubility and moisture were performed in duplicate for each sample obtained in the factorial program. Two replicates of the entire experiment were performed in the center of the program to evaluate the error.

4. Spectral Characterization

4-1. IR and UV-Vis Measurements

Infrared characterization was performed in transmittance mode using an Interspec 200-X FTIR equipment from Interspectrum in the 4 000-400 cm^{-1} wavenumber range. Chitosan powders were brought to constant mass before mixing with KBr and were transformed into KBr disc using a manual hydraulic press. UV-Vis spectra of both liquid and solid form samples were recorded using a spectrophotometer (Thermo Scientific, Evolution 220 model), in the 200-800 nm region.

Eq. (6) was used for the deacetylation degree determination using

Table 2. Results of chitosan physical-chemical properties from *Macropipus holsatus* crab waste

Experiment/ Sample no.	Deacetylation degree (DD), %	Deacetylation degree (DD), % by FTIR	Average molar mass, kDa	Viscosity, mL/g	Solubility, %	Moisture, %
1.	67.3±1.0	64.5±0.8	284±3	596±5	88.27±5.4	8.43±0.5
2.	70.3±0.4	74.5±0.1	243±11	522±20	90.68±0.8	8.58±0.3
3.	67.2±0.8	72.7±0.1	271±18	573±33	84.39±0.1	8.12±0.4
4.	67.2±0.8	68.9±1.1	312±5	647±8	81.37±12.5	8.61±0.1
5.	74.9±2.3	77.1±1.1	192±8	428±15	97.52±2.1	9.13±0.1
6.	82.0±1.2	82.5±0.2	194±6	432±11	98.00±0.0	9.49±1.7
7.	64.6±1.6	72.9±0.1	198±2	440±3	85.58±2.0	8.14±0.5
8.	66.3±0.8	79.2±0.2	201±4	445±8	77.60±2.3	7.21±0.8
Center (9, 10)	73.6±1.5	76.8±1.0	209±5	453±14	78.00±1.4	9.03±0.2

FTIR spectra according to Brugnerotto et al. [41].

$$DD(\%)=100-\left[\frac{(A_{1320}/A_{1420})-0.3822}{0.03133}\right] \quad (6)$$

4-2. X-ray Powder Diffractometry (XRD)

X-ray diffraction measurements of the chitosan samples were conducted to confirm the chitosan obtained and to calculate the crystallinity index. The analysis was performed using an X-ray diffractometer (Empyrean Series 2 X-Ray Diffraction System) operated at a voltage generator of 45 kV and a tube current of 40 mA. The instrument was equipped with Cu Kα radiation at λ=1.5406 Å and the samples were measured at 2θ angles of 5 to 45° in continuous mode. The step size was 0.007° and the step time was 0.5 s. For crystalline index (I_{Cr}) determination Eq. (7) was used [37].

$$I_{Cr}=\frac{I_{110}-I_{am}}{I_{110}}\times 100 \quad (7)$$

where: I_{110} represents the maximum intensity at 2θ=20°, while I_{am} represents the intensity of amorphous diffraction at 2θ=16°.

4-3. Color Analysis

For chromatic characteristics determination we used the CIE 1976 L*, a*, b* (CIELab) color space system, and calculated the whiteness using formula recommended by the National Fisheries Institute (NFI 1991) [39]. The estimation of L* (brightness or lightness), a* (redness-greenness), b* (yellowness-blueness), C* (chroma) and h (hue angle) was realized using a standard white plate (X= 94.0, Y=99.5, Z=106.4), while the whiteness index of chitosan samples was calculated according to the following equation equation [39]:

$$W=100-\sqrt{(100-L^*)^2+(a^*)^2+(b^*)^2} \quad (8)$$

RESULTS AND DISCUSSION

1. Physical-chemical Characterization of Chitosan

The results for chitosan characterization are presented in Table 2. The errors mentioned for the experimental runs 1-8 refer to the errors of the analytical measurements that may have occurred during the manipulation of the samples, while the error corresponding to the central point includes besides the already mentioned errors the contribution due to the experiment replication. The error was calculated as standard deviation.

Based on the results from Table 2, the main factors and their interaction effects were studied to determine which of the variables (factors) are most influential on the response (the deacetylation degree), to determine the level at which factors must be set and to evaluate the effects that occur with the change of one or more factors [34].

2. Study of Main Factors and their Interaction Effects

The main effects as well as the interaction effects for a full factorial experiment can be quickly estimated by determining the increase of the measured variable when the factor varies from its smallest value (−1) to its highest one (+1), meaning calculating the difference between the mean value of the measured variable at the maximum and the mean value at the minimum for each factor, $\Delta y=\bar{y}_+-\bar{y}_-$ [34].

Table 3. The main and interaction effects of chitosan samples

Factor/Model term	Estimated effect			Percent contribution, %		
	DD, %	$\overline{M}_w$, kDa	Solubility, %	DD	$\overline{M}_w$	Solubility
A (contact time)	2.86	1.22	−2.03	7.03	0.02	2.23
B (NaOH solvent-to-solid ratio)	−7.21	17.55	−11.38	44.68	3.92	70.26
C (NaOH concentration, %)	4.04	−81.11	3.50	14.06	83.78	6.63
AB	−2.01	20.69	−3.47	3.46	5.45	6.53
AC	1.54	1.13	−1.72	2.03	0.02	1.61
BC	−5.74	−10.80	−4.79	28.33	1.49	12.43
ABC	−0.68	−20.46	−0.76	0.40	5.33	0.31

Table 3 presents the effects and the contribution of each factor in the variation of DD, average molar mass and solubility. Viscosity highly depends on the average molar mass, therefore was not included in calculations of the factor effects. At the same time, moisture, another characteristic of chitosan, was not included because it highly depends on the atmospheric conditions.

According to Table 3, factor C (NaOH concentration) has high positive effect upon the deacetylation degree (increased NaOH concentration will favor the deacetylation degree), but a negative effect upon the average molar mass. Factor B (NaOH solvent-to-solid ratio) has a important negative effect on the solubility (the increase of factor B implies a decrease in solubility) and also a negative high effect upon the deacetylation degree. The factor interaction effects are also estimated. Their influence is less important, only BC interaction proves a significant influence on the deacetylation degree and solubility.

The main effects plots presented in Fig. 3 were realized using Minitab® 18 Statistical Software (v. 18.1, ©2017, Minitab Inc., U.S.). From Fig. 3(c) it can be seen that DD and solubility are influenced in the same way by factors B and C, while in the case of molar mass the contact time has almost no influence and the factor *A* becomes significant only if the interactions effects are considered. As the DD is the most important characteristic in the study of chitin conversion to chitosan a more detailed evaluation of the deacetylation process and the influence of operating parameters was performed by mathematical modelling using artificial neural networks (ANN). The results presented in Table 2 for deacetylation degree using potentiometric titration were further used in this study considering the factors presented in Table 1. The ANN is a part of the complex domain known as Artificial Intelligence [42]. In the present work a multilayer neural network was used as this ANN type is

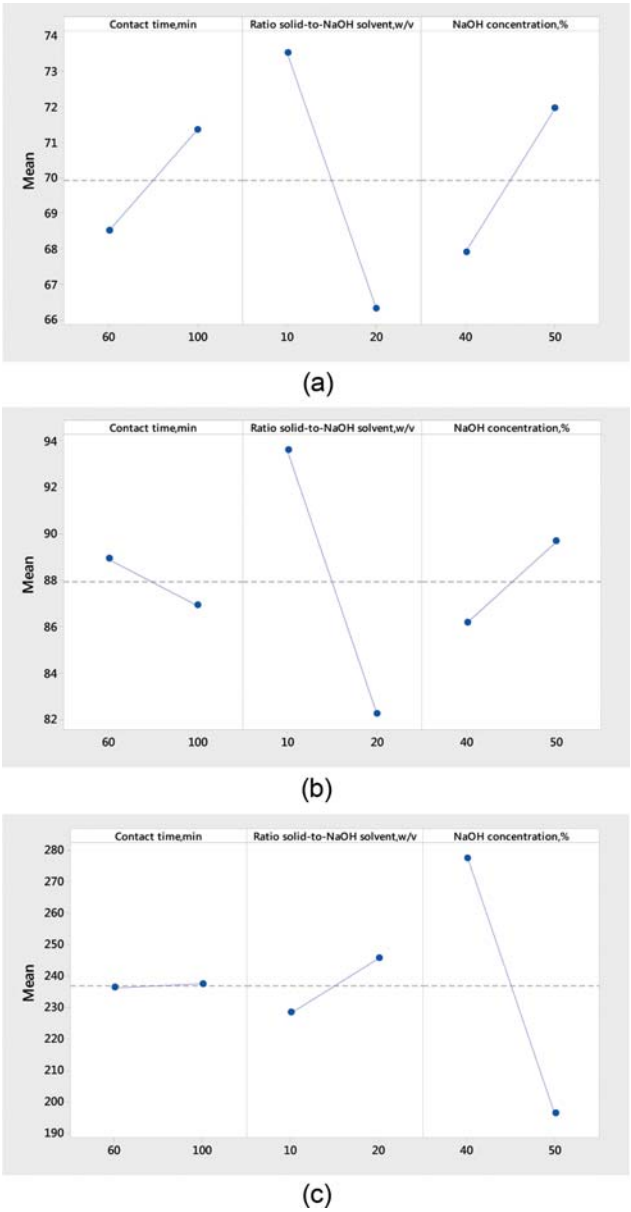

Fig. 3. Main effects plot for the analyzed physical-chemical properties of chitosan: (a) Deacetylation degree, (b) solubility and (c) average molar mass.

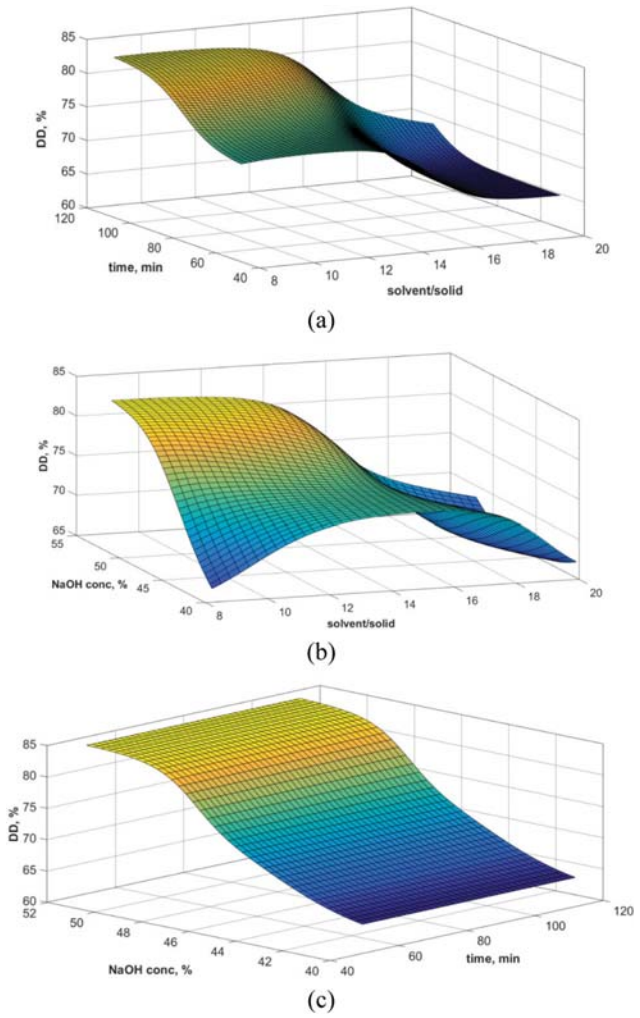

Fig. 4. (a) DD variation with time and NaOH solvent-to-solid ratio at NaOH concentration of 50%; (b) DD variation with NaOH concentration and NaOH solvent-to-solid ratio at time of 100 min; (c) DD variation with NaOH concentration and time at NaOH solvent-to-solid ratio of 10 : 1 (v : w).

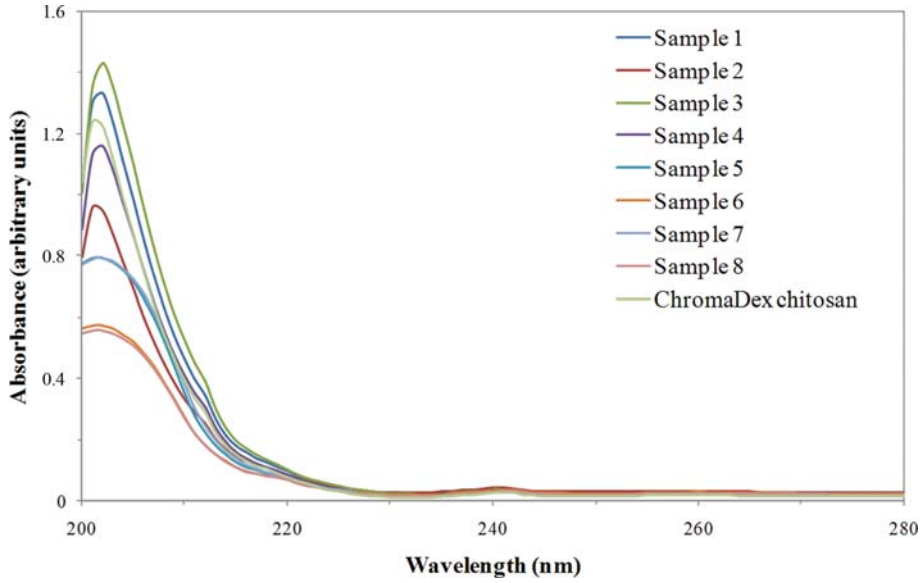

Fig. 5. UV-Vis spectra for chitosan identification.

the most used one in chemical and biochemical engineering. It is generally considered that the ANN can give a better response than classical regression, due to its generalization capacity and may be used for data outside the learning set. The architecture of the multilayer network consists in neurons (processing elements) and interneuron connections. The connection between neurons is characterized by weights. The neurons are grouped in several layers: an input layer, one or several hidden layers, and an output layer. Each layer receives signals only from previous layer and transmits results to the following layer. Minimization between actual responses of ANN and desired responses is done during the learning process by adjusting the values of the interneuron connections weights. In the learning stage the Levenberg-Marquardt algorithm (*trainlm*) was used. The ANN model was obtained in the frame of MATLAB© v15.0 (The Mathworks, Inc., Natick, Massachussetts, U.S.) considering 70 % of data samples for training and 30% for validation and testing. The best ANN topology identified during the learning process consists in an input layer (the three neurons representing the operating parameters considered), a hidden layer with three neurons and an output layer with one node, the DD. The best results obtained fit the experimental data with a determination coefficient of R^2=0.96.

The simulation of the process using the ANN put into evidence the way the deacetylation degree is influenced by the operating conditions considered and reveals an optimum value in the range of high NaOH concentrations and low solvent solid ratio (Fig. 4(a) and 4(b)).

Similarly, it could be concluded that the contact time of chitin deacetylation process (factor A) is not clearly influencing the deacetylation degree value (Fig. 4(c)).

The ANN model was further used for the optimization of operating conditions using genetic algorithms implemented in Matlab. For a population size of 100, the identified optimum coresponds to a process of deacetylation duration of 110 min, NaOH concentration of 52.0% and solvent-to-solid ratio of 9.5 : 1 (v : w) for which an optimum deacetylation degree of 83.47% can be obtained. It can be affirmed, according to Fig. 4(a), that higher durations (over 100 min) are no more essentially contributing to the increase of deacetylation degree. Therefore, the experimental conditions obtained for a duration of 100 min, a NaOH concentration of 50% and a solvent-to-solid ratio of 10 : 1 (v : w) where the deacetylation degree was 82.0±1.2% can be considered as an optimum, and, at the same time, the recommended operating conditions for obtaining chitosan samples with a relatively high deacetylation degree from crab waste.

3. Spectral Characterization

3-1. UV-Vis Characterization

UV-Vis spectral characterization was performed by dissolving chitosan samples in 0.15 M hydrochloric acid using a HCl solvent-to-solid ratio of 2500 : 1 (v : w). The spectra are presented in Fig. 5.

Fig. 5 shows a specific absorption peak at 201 nm corresponding to chitosan [35,43,44]. In all the analysed samples at 240 nm there is showed another specific peak presented as a weak absorption band assigned to $NHCOCH_3$ group contained by chitosan [45,46]. Because chitosan is a mixture of two chromophoric groups (N-acetyl-D-glucosamine and D-glucosamine), the UV-Vis data often provide insufficient information to make a clear difference between a chitin and chitosan sample [43,44]. Therefore, more spectral measurements are necessary and IR and XRD spectra are generally used in this respect.

3-2. IR Characterization

Infrared spectra of crab powder shell in sequences of initial powder, after demineralization powder and after deproteinization powder are presented in Fig. 6. To put in evidence the chitin presence, these spectra were compared with standard chitin.

M. holsatus crab shell powder presents an intense peak at 1,451 cm^{-1} which may be assigned to carbonates and another intense one at 897 cm^{-1} assigned to phosphates [47] that are naturally found in crustacea exoskeleton [6]. All spectra present two neighbor absorption bands which are less intense in the initial crab powder and become more visible after demineralization, as follows: one band at 1,707 cm^{-1} (also for standard chitin) which is assigned to C=O

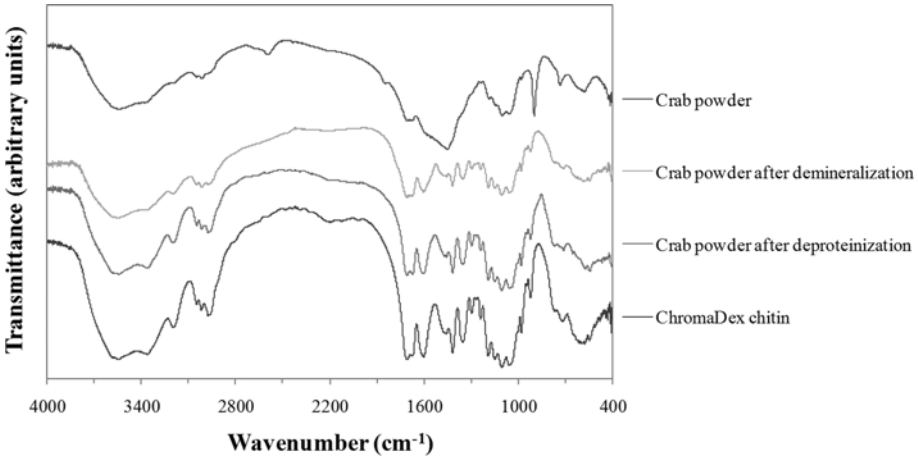

Fig. 6. IR spectra recorded for the raw material in different stages of treatment compared to standard chitin.

group hydrogen bonded to N-H of the neighboring intrasheet chain and the other band at 1,680 cm^{-1} (1,673 cm^{-1} for standard chitin) which is assigned to hydrogen bond of C=O with the hydroxymethyl group of the next chitin residue of the same chain. The above mentioned peaks and the absorption bands found for the extracted samples and also for standard chitin at 1,605 cm^{-1} (N-H bend, C-N stretch), 1,419 cm^{-1} (CH_2 ending, CH_3 deformation) and 1,353 cm^{-1} (CH bend) were noticed to be more intense after deproteinization compared with the material obtained after demineralization, which is due to the fact that most of the proteins that covered the specific bands had been removed during this stage. The results reveal the presence of α-chitin in the extracted material [48,49].

Fig. 7 presents by comparison the IR spectra recorded for the commercial chitosan and for the extracted chitosan samples. Numbers from 1 to 8 represent the samples as indicated in Table 1 and

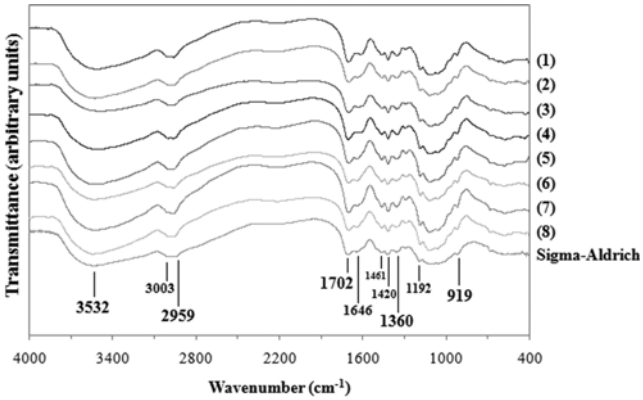

Fig. 7. IR spectra of experimentally obtained chitosan compared with a reference chitosan.

Table 4. Spectral assignments of the analyzed chitosan samples

Assignments \ Sample	Wavenumber, cm^{-1}								
	Sigma-Aldrich chitosan	1.	2.	3.	4.	5.	6.	7.	8.
$\nu(NH_2)$ assoc. in primary amines and ν(O-H) in pyranose ring [49], ν(N-H), ν(O-H), $\nu(NH_2)$ [50,51]	3532.3	3533.4	3533.2	3534.3	3534.2	3534.0	3534.9	3532.6	3532.4
ν_{as} (CH_2) in CH_2OH group [49]	3003.3	3004.4	3005.2	3001.2	3001.4	3003.2	3001.2	3003.6	3002.2
ν (C-H) [51], vibrations of CH_2 and -CH_3 groups [50], ν(C-H) in pyranose ring [49]	2959.6	2962.0	2964.8	2959.7	2961.1	2967.4	2965.1	2967.8	2966.1
ν(C=O) in $NHCOCH_3$ group [49]	1702.3	1702.6	1699.8	1700.5	1703.3	1703.1	1702.4	1703.2	1700.6
ν (NH_2) in $NHCOCH_3$ group [49], NH_2 vibration due to primary amines [51]	1646.2	1616.7	1645.4	1638.9	1639.2	1641.5	1643.7	1642.5	1642.7
$\delta(CH_2)$ in CH_2OH group [49], δ(C-H) in CH_2 [50]	1461.2	1461.4	1464.0	1463.8	1460.3	1462.4	1462.0	1462.1	1462.2
δ_s (CH_3) in $NHCOCH_3$ group [49], δ (C-H) [51]	1420.2	1418.4	1418.5	1418.9	1417.7	1418.6	1418.6	1418.7	1418.3
ν(C-N) [52], δ(CH) in pyranose ring [49]	1360.6	1358.9	1360.1	1360.3	1360.5	1361.6	1361.4	1361.2	1361.6
Complex vibrations of NHCO group [49]	1296.3	1297.4	1295.2	1296.3	1298.1	1294.5	1291.3	1296.0	1290.7
ν_s (C-O-C) glycosidic [49]	1192.9	1186.3	1189.8	1188.0	1186.3	1185.7	1187.0	1186.5	1185.8
ν_{as} (C-O-C) glycosidic [49]	1109.1	1114.1	1116.6	1117.0	1117.5	1113.5	1116.8	1115.6	1113.6
ν(C-O) skeletal vibrations [53]	1058.9	1059.2	1061.9	1062.3	1061.7	1063.7	1064.5	1063.5	1061.5
Pyranose ring skeletal vibrations [49]	919.2	923.5	922.1	923.6	923.7	921.0	920.5	921.8	921.1

Table 2.

The most important bands of the IR spectra for chitosan are found at 3,532-3,535 cm^{-1} and the molecules vibrations are assigned to the stretching vibrations of O-H and NH_2 [50,51]. The band at 3,001-3,004 cm^{-1} is assigned to CH_2 stretching vibrations from CH_2OH group [49]. The C-H stretching vibrations are found between 2,959-2,968 cm^{-1} [49,51] while the bands at 1,699-1,703 cm^{-1} are attributed to the C=O stretching vibrations from $NHCO-CH_3$ group [49]. Other important bands are found at 1,639-1,646 cm^{-1} for the NH_2 stretching vibrations from $NHCOCH_3$ group and from the primary amine groups [49,51], at 1,461-1,464 cm^{-1} which can be attributed to C-H deformation in CH_2 group [50]. The bands observed at 1,418-1,420 cm^{-1} are assigned to CH_3 deformations in $NHCOCH_3$ groups [49]. The C-N stretching is shown by the band at 1,358-1,362 cm^{-1} [52], while the glycosidic C-O-C bond is seen at 1,186-1,193 cm^{-1}. The skeletal vibrations of pyranosic ring is responsible for the band at 919-924 cm^{-1} [49].

Table 4 summarizes all these bands and puts in evidence that the operating conditions affect the obtained material and may determine small shifts. The most important shift is observed in Sample 1 for the peak at 1,616 cm^{-1} which is found at higher wavenumber in the IR spectra of the other samples. This important shift could be correlated with the smallest value of the deacetylation degree by FTIR method (Table 2) showing that the conditions of chitin deacetylation process in this case are not as effective as for the other experiments.

3-3. X-ray Powder Diffractometry

XRD measurements were used for crystallinity index determination of chitin and chitosan extracted samples. As expected, the sharpness of the chitin band is higher than the band obtained for chitosan [54]. The standard chitin sample showed peaks at 9.3°, 12.7°, 19.2°, 20.8°, 23.4° and 26.4°, while chitin after demineralization and deproteinization treatment showed peaks at 9.2°, 12.7°, 19.2°, 20.8°, 22.0°, 23.4°, 24.2°, 26.6°, 27.8° and 36.5° (Fig. 8). Among these peaks, the ones at 9.3° and 19.2° for standard chitin and the ones at 9.2°, 19.2°, 20.8°, 26.6° and 27.8° for the extracted chitin were observed to be more intense than the others. Other studies identified similar peaks for α-chitin [37,55]. The calculated value of the crystallinity degree for standard chitin was 84.0%, for chitin after demineralization was 73.4% and for chitin after deproteinization treatment was 71.5%, which are comparable with other studies [50,55,56].

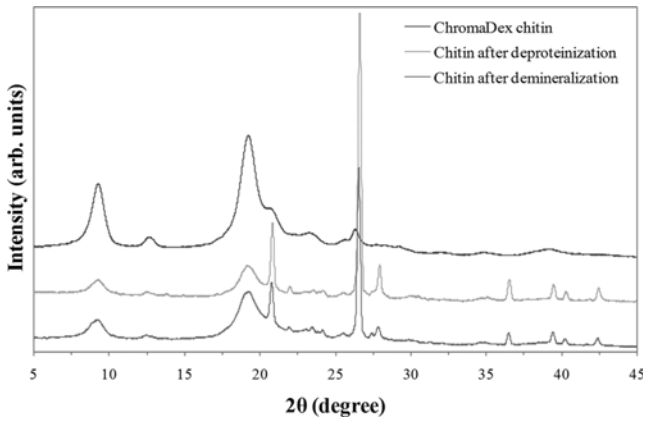

Fig. 8. XRD patterns of α-chitin samples compared with a standard chitin from ChromaDex.

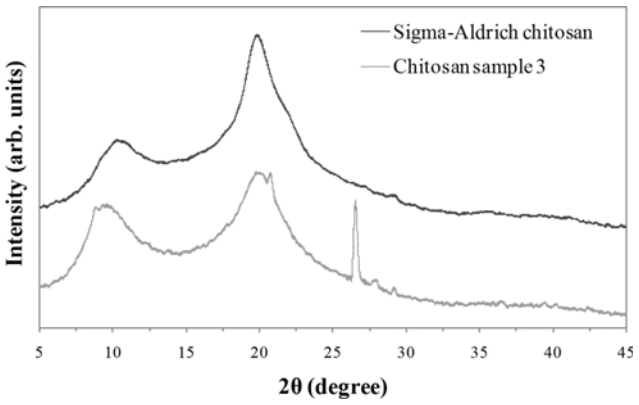

Fig. 9. XRD patterns of the extracted chitosan (sample 3) compared with a reference chitosan from Sigma-Aldrich.

For the chitosan samples, peaks at 10.5° and 19.9° for the reference chitosan and at 9.6°, 20.0°, 20.8° and 26.6° for the extracted chitosan (sample 3) were identified (Fig. 9). The calculated crystallinity index for the reference chitosan was 50.7% and for the chitosan sample was 42.0%, the results being comparable with those obtained by Pires et al. [56]. As a result of deacetylation, the crystalline peaks shifted to a slightly higher 2θ angle [57], from 9.2° to 9.6° and from 19.2° to 20.0°.

The deacetylation treatment led to the production of a less crystalline material, according to the obtained crystalline index values. The peaks indicated at 20.8°, 26.6° and 36.5° for chitin and 20.8° and 26.6° for chitosan may be due to the presence of silica traces [58,59].

The information obtained from the diffraction and the spectroscopic analyses reflects the modifications of the polymer after each of the applied treatments [60], and the XRD spectra showed that the increase of deacetylation degree leads to a decrease of crystallinity index [61]. At the same time, the deacetylation process affects the primary structure, the physical structure and the morphology of chitosan which results in a change of chain conformation and crystalline packing [60]. Thus, any factor which inflences the deacetylation degree will influence the crystalinity index.

4. Color Analysis

All the results of the chromatic characteristics for the analyzed chitosan samples are presented in Table 5 and were measured for D65/10 illuminant.

Analyzing the results presented in Table 5, it can be affirmed that, as expected, all the samples present a yellowish hue, the highest value being obtained for the Sigma-Aldrich chitosan. At the same time, the obtained L*a*b* values are similar, revealing that the operating conditions have no significant influence on the chitosan color. Comparing the whiteness values obtained for the extracted chitosan and for the commercial chitosan with those obtained by Sarbon et al. [62] from the mud crab (62.10±7.02%), it can be concluded that the chitosan obtained in the present study is slightly more white. The obtained whiteness values are higher than that

Table 5. Results of the chromatic characteristics of the chitosan samples and whiteness index

Sample	L*	a*	b*	C*	h*	Whiteness
1.	66.5±1.3	1.1±0.2	8.4±0.8	8.5±0.8	82.2±1.0	65.4±1.1
2.	67.6±1.7	1.6±0.1	10.5±0.6	10.6±0.6	81.5±0.4	65.9±1.7
3.	71.5±0.9	1.1±0.1	8.1±0.4	8.2±0.4	82.3±0.5	70.3±0.8
4.	69.8±1.3	0.9±0.2	7.3±0.9	7.3±0.9	82.8±1.1	68.9±1.1
5.	69.5±0.6	0.3±0.6	9.1±0.3	9.1±0.3	87.8±3.7	68.2±0.5
6.	69.0±0.4	0.4±0.3	8.0±0.7	8.0±0.7	87.3±1.9	68.0±0.3
7.	68.7±0.9	0.3±0.4	6.9±0.4	6.9±0.4	86.9±3.6	67.9±0.9
8.	67.9±0.3	0.1±0.5	6.6±0.9	6.6±0.9	89.6±3.8	67.2±0.4
Sigma-Aldrich chitosan	72.7±0.8	0.1±0.9	18.3±1.6	18.4±1.5	89.6±2.9	67.1±0.8
ChromaDex chitosan	75.2±1.7	1.4±1.3	8.1±0.9	8.2±1.1	80.7±8.1	73.9±1.7
ChromaDex chitin	82.0±0.8	0.7±0.4	5.3±0.3	5.4±0.2	82.5±4.5	81.2±0.8

obtained by Fernandez-Kim [39], who reported a value for whiteness index of 31.9% when a similar extraction procedure was used for chitosan extraction from crawfish.

CONCLUSIONS

The influence of three important factors on the deacetylation process (NaOH concentration, NaOH solvent-to-solid ratio and the contact time of solvent with chitin) was studied for chitosan extraction from waste of *Macropipus holsatus* crab species. The characteristics of the obtained chitosan varied due to the modifications in the deacetylation treatment, suggesting that the deacetylation parameters have a significant importance. The obtained chitosan was identified using spectral methods and colour analysis.

Using statistical analysis, ANN modelling and genetic algoritm optimization, the optimal operating conditions for chitin decetylation were identified: 100 min reacion time using NaOH solution of 50% in a solvent-to-solid ratio of 10 : 1 (v : w). The chitosan obtained under these conditions has a deacetylation degree of 82.0± 1.2%, a medium molar mass and good solubility properties.

REFERENCES

1. M. Ul-Islam, N. Shah, J. H. Ha and J. K. Park, *Korean J. Chem. Eng.*, **28**, 1736 (2011).
2. Z. Afsarian and Y. Mansourpanah, *Korean J. Chem. Eng.*, **35**, 1867 (2018).
3. S. D. Ippólito, J. R. Mendieta, M. C. Terrile, C. V. Tonón, A. Y. Mansilla, S. Colman, L. Albertengo, M. S. Rodríguez and C. A. Casalongué, in *Biological activities and application of marine polysaccharides*, E. A. Shalaby (Ed.), Intech Open, Croatia (2017).
4. F. R. De Abreu, S. P. Campana-Filho, *Polímeros: Ciência e Tecnologia*, **15**, 79 (2005).
5. H. S. Kim, M.-R. Park, S.-K. Kim and G.-T. Jeong, *Korean J. Chem. Eng.*, **35**, 1290 (2018).
6. M. H. Struszczyk, *Polimery*, **47**, 316 (2002).
7. E. S. de Alvarenga, in *Biotechnology of Biopolymers*, M. Elnashar Ed., IntechOpen, Croatia (2011).
8. G. A. M. Ruiz and H. F. Z. Corrales, in *Biological Activities and Application of Marine Polysaccharides*, E. A. Shalaby (Ed.), Croatia, InTech Open (2017).
9. O. C. Wilson Jr. and T. Omokanwaye, in *Biopolymer Nanocomposites: Processing, properties and applications*, A. Dufresne (Ed.), R. F. Grossman and D. Nwabunma (Series Eds.), Wiley Series On Polymer Engineering and Technology (2013).
10. G. Lodhi, Y.-S. Kim, J.-W. Hwang, S.-K. Kim, Y.-J. Jeon, J.-Y. Je, C.-B. Ahn, S.-H. Moon, B.-T. Jeon and P.-J. Park, *BioMed Res. Int.*, **2014**, 654913 (2014).
11. M. H. Dehghani, A. Zarei, A. Mesdaghinia, R. Nabizadeh, M. Alimohammadi and M. Afsharnia, *Korean J. Chem. Eng.*, **34**, 757 (2017).
12. H.-J. Choi and S.-W. Yu, *Korean J. Chem. Eng.*, **35**, 2198 (2018).
13. X. Lin, L. Wang, S. Jiang, L. Cui and G. Wu, *Korean J. Chem. Eng.*, **36**, 1102 (2019).
14. S. Karimidost, E. Moniri and M. Miralinaghi, *Korean J. Chem. Eng.*, **36**, 1115 (2019).
15. J. Pan, Z. Ou, L. Tang and H. Shi, *Korean J. Chem. Eng.*, **36**, 729 (2019).
16. F. Ardeshiri, A. Akbari, M. Peyravi and M. Jahanshahi, *Korean J. Chem. Eng.*, **36**, 255 (2019).
17. N. N. Bahrudin and M. A. Nawi, *Korean J. Chem. Eng.*, **36**, 478 (2019).
18. Z. Li, Z. Ma, Y. Xu, X. Wang, Y. Sun, R. Wang, J. Wang, X. Gao and J. Gao, *Korean J. Chem. Eng.*, **35**, 1716 (2018).
19. F. A. Ahing and N. Wid, *Int. J. Adv. Appl. Sci.*, **3**, 31 (2016).
20. R. F. Weska, J. M. Moura, L. M. Batista, J. Rizzi and L. A. A. Pinto, *J. Food Eng.*, **80**, 749 (2007).
21. K. E. Tokatli and A. Demirdöven, *J. Food Process. Preserv.*, **42**, e13494 (2017).
22. A. Percot, C. Viton and A. Domard, *Biomacromolecules*, **4**, 12 (2003).
23. B. B. Seghir and M. H. Benhamza, *J. Food Measurement and Characterization*, **11**, 1137 (2017).
24. N. D. Takarina, A. A. Nasrul and A. Nurmarina, *Int. J. Pharma Medicine and Biological Sciences*, **6**, 16 (2017).
25. M. Djaeni, *Reaktor*, **7**, 37 (2003).
26. F. Boßelmann, P. Romano, H. Fabritius, D. Raabe and M. Epple, *Thermochim. Acta*, **463**, 65 (2007).
27. S. H. Lv, in *Biopolymers and Biotech Admixtures for Eco-Efficient Construction Materials*, F. Pacheco-Torgal, V. Ivanov, N. Karak and

H. Jonkers Eds., Elsevier (2016).
28. E. Szymańsk and K. Winnicka, *Mar. Drugs*, **13**(4), 1819 (2015).
29. I. Younes and M. Rinaudo, *Mar. Drugs*, **13**(3), 1133 (2015).
30. I. Desportes and J. Schrével, in *Treatise on Zoology - Anatomy, Taxonomy, Biology. The Gregarines - Vol. II*, Desportes I. and Schrével J. (Eds.), BRILL (2013).
31. R. Ingle, in *Crayfishes, Lobsters and Crabs of Europe: An Illustrated Guide to common and traded species*, R. Ingle Ed., Springer Science and Business Media (2012).
32. M. C. Băcescu, *Fauna Republicii Socialiste România: Vol. IV: Crustacea. Fascicula 9: Decapoda*, Editura Academiei Republicii Socialiste România, București (1967).
33. K. E. Carpenter and N. De Angelis, in *The living marine resources of the Eastern Central Atlantic. Volume 1: Introduction, crustaceans, chitons and cephalopods*, K. E. Carpenter, N. De Angelis (Eds.), Rome (2014).
34. D. C. Montgomery, *Design and Analysis of Experiments*, 8th Ed., John Wiley & Sons, Inc., Arizona State University (2013).
35. R. Czechowska-Biskup, D. Jarosińska, B. Rokita, P. Ulański and J. M. Rosiak, *Prog. Chem. Appl. Chitin and Its Derivatives*, **XVII**, 5 (2012).
36. J. B. Dima, C. Sequeiros and N. Zaritzky, in *Biological Activities and Application of Marine Polysaccharides*, E. A. Shalaby (Ed.), Intech (2017).
37. F. A. Al Sagheer, M. A. Al-Sughayer, S. Muslim and M. Z. Elsabee, *Carbohydr. Polym.*, **77**, 410 (2009).
38. W. Wang, S. Bo, S. Li and W. Qin, *Int. J. Biol. Macromol.*, **13**, 284 (1991).
39. S.-O. Fernandez-Kim, Louisiana State University Master's Thesis (2004).
40. AOAC 2000 standard, *Determination of moisture content*.
41. J. Brugnerotto, J. Lizardi, F. M. Goycoolea, W. Argüelles-Monal, J. Desbrières and M. Rinaudo, *Polymer*, **42**, 3578 (2001).
42. D. R. Baughman and Y. A. Liu, *Neural Networks in Bioprocessing and Chemical Engineering*, Academic Press, San Diego (1995).
43. J. Kumirska, M. Czerwicka, Z. Kaczyński, A. Bychowska, K. Brzozovski, J. Thöming and P. Stepnovski, *Mar. Drugs*, **8**, 1589 (2010).
44. Y. Liu, Y. Bai and H. Liu, in *Handbook of Analysis of Active Compounds in Functional Foods*, L. M. L. Nollet and Fidel Toldra (Eds.), CRC Press (2012).
45. J. Csaszar and N. M. Bizony, *Acta Physica et Chemica*, **31**, 730 (1985).
46. S. Gaisford, in *Aulton's Pharmaceutics: The Design and Manufacture of Medicines*, M. E. Aulton and K. M. G. Taylor (Eds.), 5th Ed., Elsevier (2018).
47. A. T. Balaban, M. Banciu and I. I. Pogany, *Aplicații ale metodelor fizice în chimia organică*, Ed. Științifică și Enciclopedică, București (1983).
48. M. Rinaudo, *Prog. Polym. Sci.*, **31**, 608 (2006).
49. M. Kaya, T. Baran, A. Mentes, M. Asaroglu, G. Sezen and K. O. Tozak, *Food Biophysics*, **9**, 145 (2014).
50. H. E. Knidri, R. Belaabed, R. E. Khalfaouy, A. Laajeb, A. Addaou and A. Lahsini, *JMES*, **8**, 3648 (2017).
51. I. K. D. Dimzon and T. P. Knepper, *Int. J. Biol. Macromol.*, **72**, 939 (2015).
52. E. M. Dahmane, M. Taourirte, N. Eladlani and M. Rhazi, *Int. J. Polym. Anal. Charact.*, **19**, 342 (2014).
53. R. S. C. M. Q. Antonino, B. R. P. L. Fook, V. A. O. Lima, R. I. F. Rached, E. P. N. Lima, R. J. S. Lima, C. A. P. Covas and M. V. L. Fook, *Marine Drugs*, **15**, 8 (2017).
54. A. Alishahi, A. Mirvaghefi, M. R. Tehrani, H. Farahmand, S. A. Shojaosadati, F. A. Dorkoosh and M. Z. Elsabee, *J. Polym. Environ.*, **19**, 781 (2011).
55. L. Zelencova, S. Erdoğan, T. Baran and M. Kaya, *Polym. Sci. - Ser. A*, **57**, 440 (2015).
56. C. T. G. V. M. T. Pires, J. A. P. Vilela and C. Airoldi, *Procedia Chem.*, **9**, 222 (2014).
57. M. Ioelovich, *Res. Rev.: J. Chem.*, **3**, 7 (2014).
58. NIOSH Manual of Analytical Methods (NMAM), Silica Crystalline by XRD, 4th Ed., method 7500 (2003).
59. Standard X-ray Diffraction Powder Patterns, NBS Monograph 25, section 18 (S18), U.S. Department of Commerce/National Bureau of Standards (1981).
60. B. Focher, A. Naggi, G. Torri, A. Cosani and M. Terbojevich, *Carbohydr. Polym.*, **18,** 43 (1992).
61. Y. Zhang, C. Xue, Y. Xue, R. Gao and X. Zhang, *Carbohydr. Res.*, **340**(11), 1914 (2005).
62. N. M. Sarbon, S. Sandanamsamy, S. F. S. Kamaruzaman and F. Ahmad, *J. Food Sci. Technol.*, **52**(7), 4266 (2014).